Liquid metal based magnetic cooling: velocity measurements

Lei, Z.; Raebiger, D.; Eckert, S.; Eckert, K.;

Originally published:

July 2017

Magnetohydrodynamics 53(2017)2, 403-410

Perma-Link to Publication Repository of HZDR:

https://www.hzdr.de/publications/Publ-25761

LIQUID METAL BASED MAGNETIC COOLING: VELOCITY MEASUREMENTS

Z. Lei[1,2], *D. Raebiger*[2], *S. Eckert*[2], *K. Eckert*[1,2]

[1] *Chair of Transport Processes at Interfaces, Technische Universität Dresden, D-01062 Dresden, Germany*

[2] *Helmholtz-Zentrum Dresden–Rossendorf, Bautzner Landstrasse 400, 01328 Dresden, Germany*

e-Mail: Zhe.Lei@tu-dresden.de; Kerstin.Eckert@tu-dresden.de

Heat transfer enhancement in a segment of the active magnetic regenerator (AMR), consisting of a magnetocaloric material (Gadolinium) and a heat transfer fluid in between, which is periodically magnetized and demagnetized, is investigated in this work. After giving a brief account on how magnetohydrodynamic (MHD) convection can be used to enhance the heat transfer from flat plate gadolinium toward the heat transfer fluid we apply two different techniques for MHD flow generation. In the first approach, an electric current I was injected into an electrically conducting, aqueous heat transfer fluid (NaOH). A heat transfer enhancement of about 40% (I=3 mA) was found by means of a Mach-Zehnder interferometer. In the second approach, a liquid metal (GaInSn) was used which is potentially an interesting candidate for a heat transfer fluid in an AMR operating with high cycling frequency. Velocity measurements by means of ultrasound doppler velocimetry with a quasi uniform static magnetic field (220 mT) in the gadolinium channel are presented.

Introduction. Magnetic cooling (MC) is an alternative cooling technology that possesses several advantages, such as the use of an environmentally friendly heat transfer fluid and a non-toxic solid cooling material. The latter allows a compact design and a more silent operation as the compressor is replaced with the magnet and the only moving part could either be the magnet or the regenerator bed. Principally, this is realized by the magnetocaloric effect (MCE), employing a magnetocaloric material (MCM) [1]. Since the introduction of the a ctive magnetic regenerator (AMR) principle, based on the work of [2], more than 62 magnetic cooling prototype devices have been built and corresponding simulation tools been developed [3].

Comparing the current efficiency of magnetic cooling with conventional refrigeration, room-temperature MC is still far from being competitive. This is partly due to the fact that the efficiency of the AMR is strongly coupled to the efficiency of the convective heat transfer in the regenerator. Hence, optimizing the performance of the AMR is of primary importance. The main objectives consist in predicting the temperature span between the hot and the cold end of the AMR and its cooling capacity as a function of the time, the frequency of operation, the utilization or the thermal losses. Experimental approaches to determine the temperature span and the cooling capacity in different MCM geometries are discussed in [4]. Despite these efforts, insufficient heat transfer is currently one major bottleneck of the AMR. This is particularly true at the desired high power density to develop compact and economic MC devices, because the fluid flow through the active regenerator is oscillatory.

Therefore, this work introduces first a heat transfer enhancement method by means of magnetohydrodynamic (MHD) convection using an aqueous heat transfer fluid. This type of convection is driven by the action of the Lorentz force density,

$\mathbf{f}_\mathrm{L} = \mathbf{j} \times \mathbf{B}$, generated by the interaction between an electric current density $\mathbf{j}$ and a magnetic flux density $\mathbf{B}$. The realization of this idea during MC is relatively cheap, especially, during the magnetization phase, as the electric energy required is small and the magnetic field is already available. For this purpose, we applied an experimental setup sufficiently simplified with respect to the magnetic field and current injection such that it is still possible to measure both the velocity and the temperature field. By means of particle image velocimetry and Mach-Zehnder interferometery [5, 6] we are able to deliver for the first time a proof-of-principle of heat transfer enhancement in MC by MHD flows.

The next part is devoted to experiments in which the aqueous heat transfer liquid is replaced by a liquid metal (GaInSn), pumped through the gadolinium (Gd) channel. Based on its small Prandtl number, GaInSn is expected to be a promising candidate for a heat transfer fluid in a high cycling frequency (rotating) AMR. We report on ultrasound Doppler velocity measurements in GaInSn during the magnetization stage of the channel as well as in 0.5 M NaOH aqueous solution for comparison.

1. Experiments.

1.1. Aqueous heat transfer fluid. Gadolinium (Gd99.5% pure, Jiangxi South Rare Earth Hi-Tech Co., Ltd.) is used as a magnetocaloric material. It was machined to a flat plate with an area of $9.6 \times 9.6\,\mathrm{mm}^2$ and a thickness of 0.72 mm. After polishing the surface to a roughness of less than 0.01 mm, the plate was glued to one side of a cuboid quartz glass cuvette with an inner side length of 10 mm, as shown in Fig. 1*a*, and is in a uniform electrical contact with the electrolyte. Due to the small temperature difference between the Gd plate and the surrounding ambient air together with the low thermal conductivity of the air, the heat loss to the surrounding can be neglected.

Two NdFeB permanent magnets were combined to form a non-uniform magnetic field to generate the MHD flow and to trigger the magnetocaloric effect of the Gd plate. For this purpose, two rectangular block magnets ($50 \times 30 \times 12\,\mathrm{mm}^3$) were juxtaposed with opposite magnetization directions so that their smallest sides

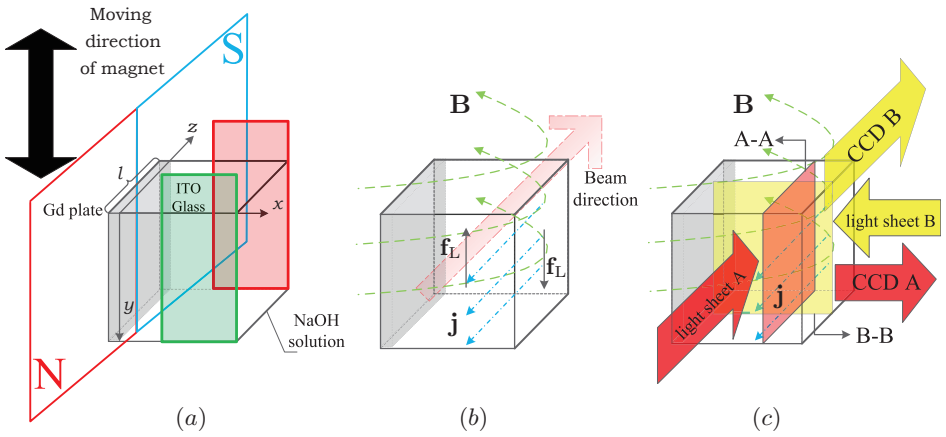

Fig. 1. (*a*) Schematic illustration of the experimental setup and (*b*) the position of the cell with respect to the laser beam of the Mach-Zehnder interferometer. Additionally, the orientation of magnetic induction, current and Lorentz force density is plotted in (*b*). In (*c*) the positions of the light sheets are shown to measure the primary flow in the A-A plane (light sheet A) and the secondary flow in the B-B-plane (light sheet B) by means of the particle image velocimetry.

touched at the outer side of the glass cell at the middle of the Gd plate (cf. Fig. 1*a*). The magnetic field was simulated using a 3D finite element method together with Ampere's law. The simulation show the expected quasi 2D magnetic field distribution in the entire cell region [6], sketched by the green arrows in Fig. 1b. The magnet assembly just described was mounted on a 1D motorized linear translation stage which was moved with a speed of 10 mm/s during the magnetization and demagnetization phases along the y-direction (cf. Fig. 1*a*).

Two transparent electrodes made of indium–tin oxide (ITO) glass are placed parallel to each other on the opposite sides of the cell along the beam direction (cf. Fig. 1*a*). They are connected to an electro-chemical workstation (CHI 660C). By means of injecting a defined electric current into the solution, MHD convection is generated. As an electrolyte, which also acts as a heat transfer fluid, NaOH solution with a concentration of 0.5 mol/L is used. The Joule heat received by the heat transfer fluid is negligible. Taking 3 mA of electric current input as an example, the heat generated could be calculated via $\mathrm{d}Q/\mathrm{d}t = I^2R$ [W], where I is the electric current and R is the electric resistance of the fluid. The electric resistance is defined by $R = \rho \cdot l/A$, where ρ is the electric resistivity, l is the length and A is the cross-section area. Taking the electric conductivity 9.3 S/m for 0.5 M NaOH solution, the resulting Joule heat is less than 0.0001 W and the overall thermal energy pumped into the liquid in 5 s is less than 0.5 mJ, i.e. 1% of the energy transfered into the fluid by the magnetocaloric effect (see Fig. 4*b*).

The velocity field of MHD convection inside the heat transfer fluid is measured by means of particle image velocimetry (PIV), as illustrated in Fig. 1*c*. For this purpose, the NaOH solution was seeded with buoyancy-neutral polystyrene particles (9.6 μm mean diameter, microparticles GmbH).

1.2. Galinstan as a heat transfer fluid. Gadolinium of the same supplier was machined after the same polishing procedure to a flat plate with an area of $50 \times 10\,\mathrm{mm}^2$ and a thickness of 0.8 mm. This plate was embedded inside a plexiglass channel, as shown in Fig. 2.

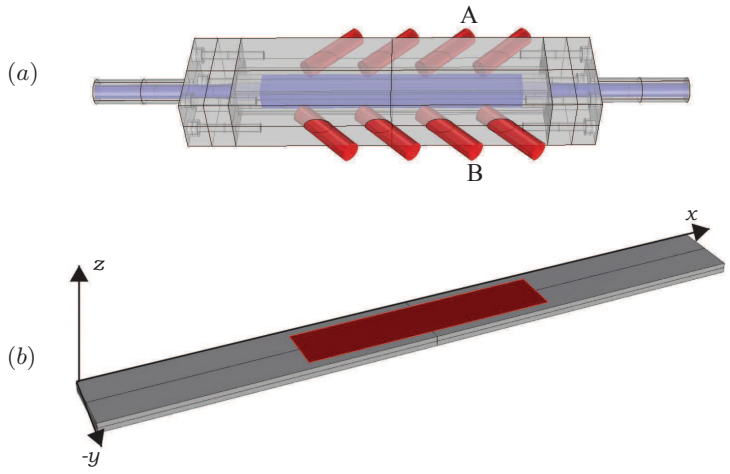

Fig. 2. (*a*) Schematic illustration of the experimental channel with a cross-sectional area of 10×10 mm. The red cylinder represent the positions, where the UDV transducer is mounted with an angle of 45 degree with respect to the x-direction. Eight UDV transducers can be used in total, where the remaining four are located at the back side of the channel. (*b*) Position of the Gd plate in the top wall.

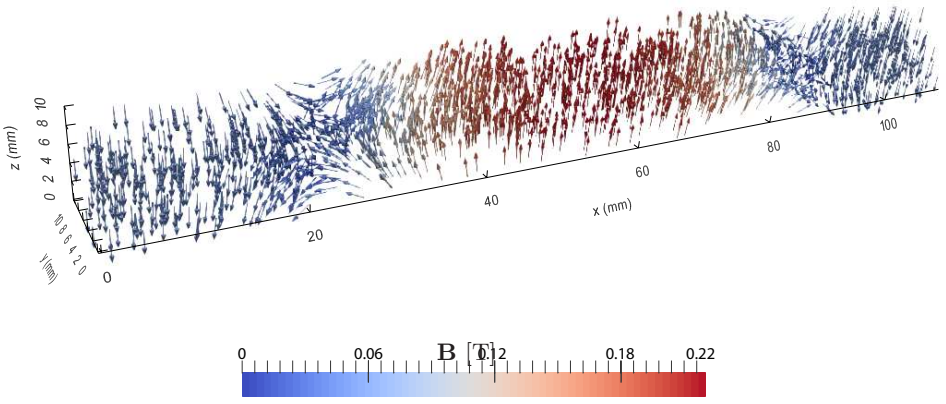

Fig. 3. Magnetic flux density distribution simulation of the NdFeB magnet ensemble used in the Galinstan channel flow: the color bar shows the magnitude and the arrows refer to the vector of magnetic flux density indicating a 3D distribution in the area of the main channel (cross-section $10\times10\,\mathrm{mm}^2$) shown in Fig. 2*a*.

Instead of a water-based heat transfer fluid, the plexiglass channel is filled with a liquid metal for which Galinstan (GaInSn) is used. Galinstan is pumped through the channel by means of a peristaltic pump.

Ultrasound doppler velocimetry (UDV) [7, 8] is used to measure the velocity distribution in the channel by ultrasound transducers. The transducers are attached to the channel at an angle of 45 degree with respect to the x-direction (see Fig. 2.)

Two permanent magnetics (supermagnets) ($50\times50\times12.5\,\mathrm{mm}^3$) with N35 magnetization are arranged such that the biggest side faces of each have a gap of 30 mm in between. Two magnets were regulated by means of a 3D printed acrylonitrile butadiene styrene plastics holder, integrated by a computer programmed electric mounting stage moving with a speed of 30 mm/s along the y-direction (see Fig. 2*b*). The magnetic field was simulated using a 3D finite element method together with Ampere's law. The simulation shows the expected quasi 2D magnetic field distribution in the entire flow region inside the duct, sketched by the blue volume in Fig. 3. A 220 mT quasi 1D uniform magnetic field anti-parallel to the z-direction is formed to trigger the magnetocaloric effect in the solid phase and to generate the MHD flow at the adjacent liquid phase.

2. Preliminary results and summary. MHD convection is driven by the Lorentz force density $\mathbf{f}_\mathrm{L} = \mathbf{j}\times\mathbf{B}$. The magnitude of the electric current density, $\mathbf{j}(\mathbf{r})$, is given by $\mid\mathbf{j}\mid = I/A_\mathrm{ITO}$, where A_ITO refers to the area of the ITO glass. In the present configuration, $\mathbf{f}_\mathrm{L}$ is mainly caused by the interaction of the z-component of $\mathbf{j}$ and by the x-component of $\mathbf{B}$. In the rear part of the cell, for $l/2 < z \leq l$, $\mathbf{B}_x < 0$, whereas $\mathbf{B}_x > 0$ in the front part for $0 \leq z < l/2$ (cf. Fig. 1*b*.) Therefore, $\mathbf{f}_\mathrm{L}$ points upwards in the front part and downwards, i.e. parallel to the positive y-direction in the rear part (Fig. 1*b*). The resulting torques in the A-A plane in Fig. 1*c* set the fluid into a swirling motion between the ITO electrodes, see Fig. 4*a*. The swirling flow causes a radial pressure gradient. As a result, a secondary flow sets in. This secondary flow has the shape of a torus [6], the axis of which emerges in the center of the A-A plane, parallel to the x-axis. At this center axis, the secondary flow is directed away from the Gd plate. By contrast, in the

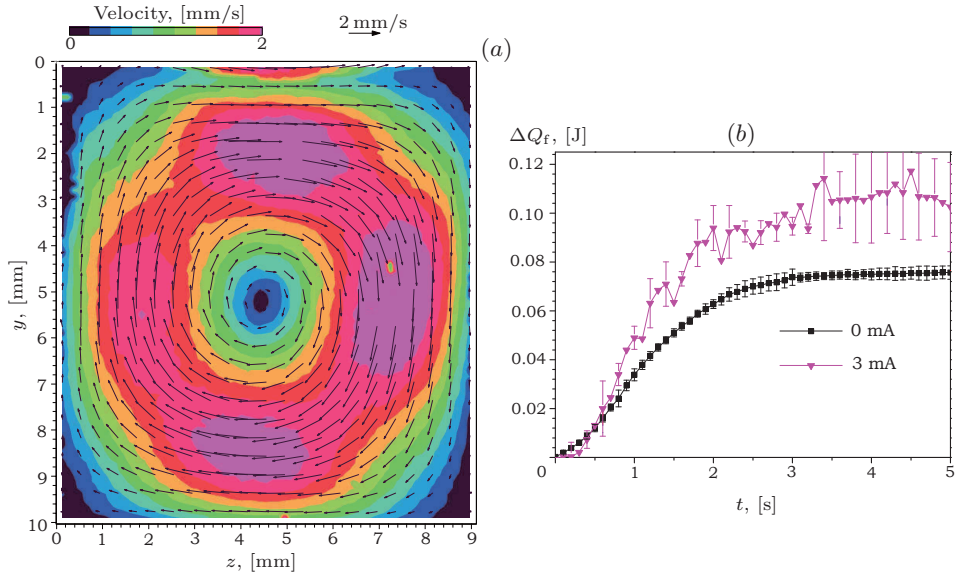

Fig. 4. (*a*) PIV measurements of the velocity field: a fully developed primary flow in the A-A plane ($I = 2\,\mathrm{mA}$), and (*b*) the measured evolution of thermal energy, ΔQ_f, transferred into the 0.5 M NaOH solution vs. the time during the magnetization phase at different levels of MHD convection expressed by the electric current I.

outer parts of the toroidal-like vortex, the flow is towards the Gd plate. Since the engine of the primary flow is between the ITO electrodes, shear forces, along with the secondary flow, are responsible for setting the remaining electrolyte volume between the ITO electrodes and the Gd plate into motion.

The 2D space-resolved temperature field in the thermal boundary layer in the vicinity of the Gd plate is measured by the Mach-Zehnder interferometer (MZI) in the region extending between $0\mathrm{mm} \le x \le 3\mathrm{mm}$ and $3\mathrm{mm} \le y \le 7\mathrm{mm}$. Each temperature point mapped in the x-y plane is an averaged along the z-direction following the optical path. Since the temperature field is not 1D, we present in Fig. 4*b* the evolution of the temperature field in terms of the thermal energy transferred into the 0.5 M NaOH solution for a 3 mA electric current input during the magnetization process. The reference case without the electric current ($I = 0$), i.e. pure thermal diffusion, is additionally plotted. The thermal energy, $\Delta Q_\mathrm{f}(t, I)$, is obtained by integrating over the temperature field $\Delta T_\mathrm{f}(x, y, t, I)$, measured by the MZI and extend to $0\mathrm{mm} \le y \le 10\mathrm{mm}$ by multiplying a factor of $N = 10/4 = 2.5$

$$\Delta Q_\mathrm{f}(t, I) = \int_{y=3\mathrm{mm}}^{y=7\mathrm{mm}} \int_{x=0\mathrm{mm}}^{x=3\mathrm{mm}} C_{p,f}\rho_\mathrm{f} V_\mathrm{f}(x, y)\Delta T_\mathrm{f}(x, y, t, I) \cdot N \mathrm{d}x\mathrm{d}y, \qquad (1)$$

where $C_{p,f} = 4.023\times10^3\mathrm{J/kg{\cdot}K}$ is the specific heat capacity, $\rho_\mathrm{f} = 1.019\times10^3\mathrm{kg/m}^3$ is the density of 0.5 M NaOH, and $V_\mathrm{f}(x, y)$ is the volume of each pixel with unit of [m]. In the presence of MHD convection, we find a significantly higher ΔQ_f transferred into the alkaline solution in the presence of a small electric current input. This means that the transfer proceeds more quickly, as seen in the 3 mA curve. Note that equilibrium is not reached at 5 sec, i.e. the ΔQ_f plateau values differ. This results from the fact that only the thermal boundary layer but not the entire fluid region is mapped. The reason for the higher standard deviation in the presence of MHD convection is the average over three independent experiments

which slightly differ in velocity field. For detailed experimental results we refer to [6].

With this work we could clearly show that MHD convection is able to significantly improve the heat transfer from the magnetocaloric material into an aqueous heat transfer fluid, with the configuration and parameters studied, provided it is electrically conducting.

We next analyze a more relevant geometry for an AMR consisting of a channel segment and a magnetocaloric material which is integrated in the sidewall (see Fig. 2). As explained, in this figure, ultrasound transducers are used to map the velocity distribution in the channel.

Preliminary result of the flow without a magnetic field are shown in Fig. 5*a*. The figure displays the profile of the x-component of the velocity processed by two transducers located at the opposite sides of the channel. The transducers used for this reconstruction are marked by A and B in Fig. 2*a*. The 45 degree orientation of the transducers with respect to the flow direction, preventing the echoes from the Galinstan-plexiglass boundary [9], is already taken into account. The data of the measurement region which is closer to the respective transducer, i.e. $y < 5$ mm for the transducer on the front side and $y > 5$ mm for the transducer on the back side of the channel (Fig. 2*a*), enter with a higher weight due to a higher signal into the noise ratio in Fig. 5a.

For the case of the vanishing magnetic field (Ha = 0, Fig. 5*a*), the expected Poiseuille profile is recovered by analogy with the measurements made with the NaOH solution (see [9]).

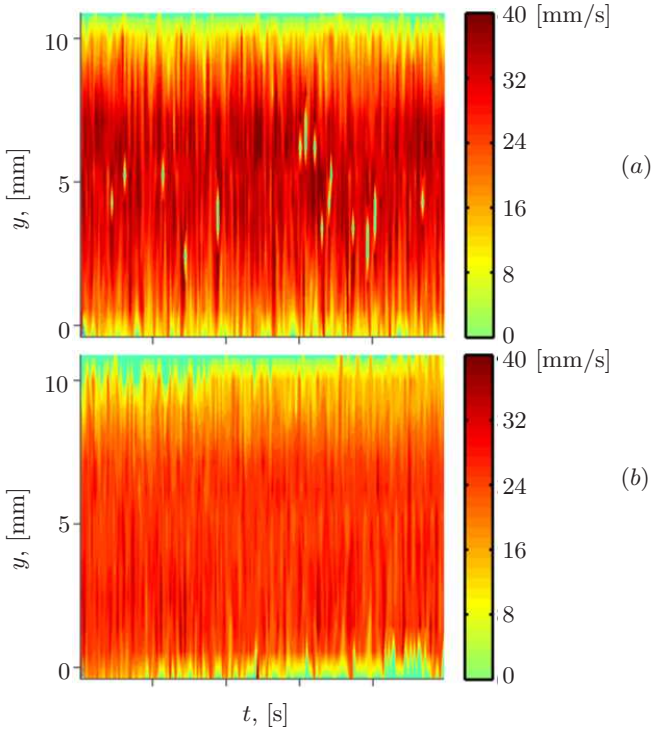

Fig. 5. The combined reconstructed velocity profile measured by UDV transducers: (*a*) without the magnetic field, and (*b*) with a static magnetic field of approximately 220 mT shown in Fig. 3.

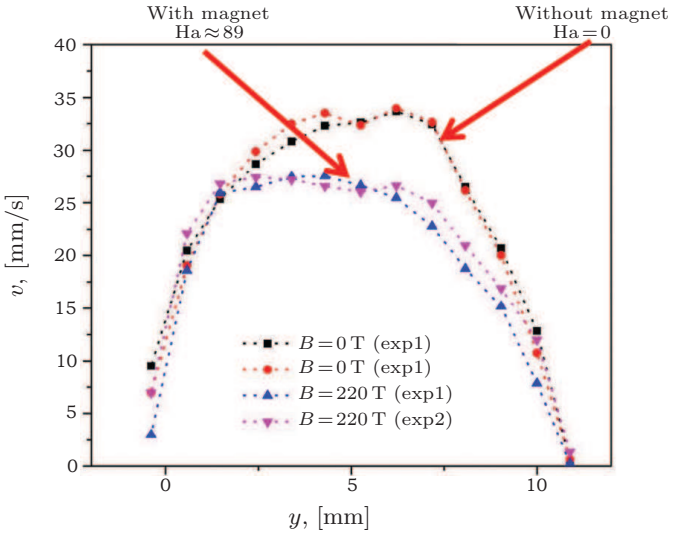

Fig. 6. The mean velocity profile obtained by averaging the velocity data over 250 s.

Based on the mean velocity component in the x-direction (Fig. 5*a*), $\mathrm{Re} = \rho v l/\mu \approx 1007$ is obtained, where $l = 0.01\,\mathrm{m}$ is the characteristic length of the flow and $\mu = \rho_{\mathrm{Galinstan}} \times \nu_{\mathrm{Galinstan}} \approx 1.90 \cdot 10^{-3}$ Pa·s is the dynamic viscosity of Galinstan; a laminar flow regime is clearly indicated. In the presence of the magnetic field plotted in Fig. 3, the Hartmann number is $\mathrm{Ha} = BL\sqrt{\sigma/(\rho\nu)} \approx 89$, where $L = l/2$ is the characteristic length and $\sigma = 3.1 \times 10^6\,\mathrm{S/m}$ is the electric conductivity of Galinstan. The velocity distribution is smoother compared to $\mathrm{Ha} = 0$ and shows a decrease in maximum velocity. The velocity distribution agrees with the theoretical analyses and numerical simulations [10] of the flow between Shercliff walls, i.e. the walls parallel to the magnetic field.

By averaging the velocity data over 250 s, the resulting mean velocity profile is plotted in Fig. 6. A good reproducibility between independent experiments exist and the no-slip boundary condition is clearly mapped by the UDV transducers. The decrease in maximum velocity magnitude for $\mathrm{Ha} = 89$ compared to the Poiseuille flow at $\mathrm{Ha} = 0$ amounts to about 20%.

If compare to a conventional Hartmann flow which was comprehensively studied in the past, the present channel configuration presents several interesting features. It possesses a transitional region in which the liquid metal both enter the magnetic field and meets a boundary condition which changes from an electrically non-conducting wall to a wall of finite conductivity. Furthermore, the magnetic field also changes in time during magnetization and demagnetization, where the speed of the magnet, $O(30\,\mathrm{mm/s})$, is of the same order of magnitude as the flow velocity. On the resulting velocity field and on the heat transfer enhancement in magnetic cooling, we will report in detail in a work in progress [11].

Acknowledgements. We thank the China Scholarship Council (CSC) for financial support for Zhe Lei's PhD at TU Dresden. We also acknowledge the support by Deutsches Zentrum für Luft- und Raumfahrt (grant no. 50WM1350). LIMTECH seed grant is acknowledged for financial support of some experimental hardware. We thank Prof. A. Kitanovski and Dr. U. Tomc for discussions on liquid metals in magnetic cooling. For further stimulating discussions, Dr. K. Timmel, T. Gundrum, T. Richter, J. Nowak, Dr. S. Günther are gratefully acknowledged.

References

[1] A. Kitanovski, P.W. Egolf.Mach- Thermodynamics of magnetic refrigeration. *International Journal of Refrigeration*, vol. 29(1) (2006), pp. 3–21.

[2] G. Brown. Magnetic heat pumping near room temperature. *Journal of Applied Physics*, vol. 47(8) (1976), pp. 3673–3680.

[3] K. Engelbrecht, G. Nellis, S. Klein. A numerical model of an active magnetic regenerator refrigeration system. In: *Cryocoolers 13, Springer*, (2005), pp. 471–480.

[4] J. Tušek, A. Kitanovski, S. Zupan, I. Prebil, A. Poredoš. A comprehensive experimental analysis of gadolinium active magnetic regenerators. *Applied Thermal Engineering*, vol. 53(1) (2013), pp. 57–66.

[5] Z. Lei, X. Yang, C. Haberstroh, B. Pulko, S. Odenbach, K. Eckert. Space- and time-resolved interferometric measurements of the thermal boundary layer at a periodically magnetized gadolinium plate. *International Journal of Refrigeration*, vol. 56 (2015), pp. 246–255.

[6] Z. Lei, C. Haberstroh, S. Odenbach, K. Eckert. Heat transfer enhancement in magnetic cooling by means of magnetohydrodynamic convection. *International Journal of Refrigeration*, vol. 62 (2016), pp. 166–176.

[7] S. Eckert, G. Gerbeth. Velocity measurements in liquid sodium by means of ultrasound doppler velocimetry. *Experiments in Fluids*, vol. 32(5) (2002), pp. 542–546.

[8] T. Vogt, D. Räbiger, S. Eckert. Inertial wave dynamics in a rotating liquid metal. *Journal of Fluid Mechanics*, vol. 753 (2014), pp. 472–498.

[9] Z. Lei, D. Raebiger, S. Eckert, K. Eckert. Liquid metal based magnetic cooling: velocity measurements. In: *Proceedings of the 10th PAMIR International Conference*, 2016.

[10] O. Zikanov, D. Krasnov, T. Boeck, A. Thess, M. Rossi. Laminar-turbulent transition in magnetohydrodynamic duct, pipe, and channel flows. *Applied Mechanics Reviews*, vol. 66(3) (2014), p. 030802.

[11] .Z. Lei, A. Kitanovski, K. Eckert (unpublished).